

# Heat Loads Due To Small Penetrations In Multilayer Insulation Blankets

W L Johnson<sup>1</sup>, K W Heckle<sup>2</sup>, and J E Fesmire<sup>3</sup>

<sup>1</sup>Glenn Research Center, Cleveland, OH, 44135 USA

<sup>2</sup>Sierra Lobo, Cryogenics Test Laboratory, Kennedy Space Center, FL 32899 USA

<sup>3</sup>Cryogenics Test Laboratory, Kennedy Space Center, FL 32899 USA

E-mail: Wesley.L.Johnson@nasa.gov

**Abstract.** The main penetrations (supports and piping) through multilayer insulation systems for cryogenic tanks have been previously addressed by heat flow measurements. Smaller penetrations due to fasteners and attachments are now experimentally investigated. The use of small pins or plastic garment tag fasteners to ease the handling and construction of multilayer insulation (MLI) blankets goes back many years. While it has long been understood that penetrations and other discontinuities degrade the performance of the MLI blanket, quantification of this degradation has generally been lumped into gross performance multipliers (often called degradation factors or scale factors). Small penetrations contribute both solid conduction and radiation heat transfer paths through the blanket. The conduction is down the stem of the structural element itself while the radiation is through the hole formed during installation of the pin or fastener. Analytical models were developed in conjunction with MLI perforation theory and Fourier's Law. Results of the analytical models are compared to experimental testing performed on a 10 layer MLI blanket with approximately 50 small plastic pins penetrating the test specimen. The pins were installed at ~76-mm spacing inches in both directions to minimize the compounding of thermal effects due to localized compression or lateral heat transfer. The testing was performed using a liquid nitrogen boil-off calorimeter (Cryostat-100) with the standard boundary temperatures of 293 K and 78 K. Results show that the added radiation through the holes is much more significant than the conduction down the fastener. The results are shown to be in agreement with radiation theory for perforated films.

## 1. Introduction

Early in the development of multilayer insulation (MLI) systems, multiple spacer materials and reflector materials were tested at the coupon level on different types of calorimeters. As the MLI systems progressed to tank applications, it was found that the heat load through the blanket systems increase by somewhere between 2 and 5 times. [1-5] These "degradations" in the tank applied blanket performance are credited to multiple different sources: penetrations of fluid lines and instrumentation lines through the blanket [6], seams [7,8], integration with structural elements of the tank, compression through the layers, and structural elements within the blanket that hold it together. Many of these effects can be directly evaluated by test at given conditions on the ground, however, the thermal environments of space, especially after leaving low earth orbit can vary widely. Thus it is desirable to numerically account for these degradations in multiple environments without having to spend the effort to test in all environments.

In 1966, Black [9] performed testing on a single 0.8 mm diameter nylon pin. The predicted heat load from that pin was 0.3 mW, but the measured change in heat load was approximately 3 mW. Similarly, Stimpson found that the localized heat load for a single button was approximately 12 mW, but only a linearized model was proposed that does not allow environmental effects to be considered. [1] To address the presence of the small pins, tags, or stitches that are often used to hold a blanket together and allow for ease of handling, a series of tests were performed both with and without these elements to allow for evaluation of performance. Additionally, simple first order thermal models were developed to allow for a broader application of the results.

## 2. Experimentation

In order to measure the thermal performance of various insulation systems, NASA Kennedy Space Center's Cryogenic Test Laboratory uses liquid nitrogen boil-off calorimetry for a variety of its instruments. This test program used the Cryostat-100 cylindrical calorimeter, which is well documented elsewhere [10-12]. The uncertainty of heat flux measurements on Cryostat-100 have been calculated to be +/- 3.2% [10]. Cryostat-100 testing yields absolute thermal performance of the multilayer insulation systems in terms of heat load ( $Q$ ). The heat load can then be normalized to the logarithmic mean surface area and converted to heat flux ( $q$ ) in accordance with ASTM C1774, Annex A1. [13]

The objectives of the testing were to measure the thermal performance small penetrations in the form of nylon pins. To determine the net effect, it was determined that using one tag would not cause enough thermal disturbance in the blanket. Initial calculations assuming a 2 mm diameter by 38 mm long pin suggested that placing approximately 40 pins in a blanket would produce a heat load increase of 0.25 W. Because initial testing had shown a heat load of approximately 0.31 W, this amount would almost double the heat load through the blanket and give a more accurate result. Based on this analysis, pins every 76 mm was determined to be the most regular pattern to give approximately 40 pins in the blanket.

For the sake of repeatability of blanket performance, it was decided to use a 10 layer Integrated Multi-Layer Insulation (IMLI) blanket that had been previously tested both by itself (A164) [14] and in multiple hybrid configurations (A174, A175, A181, and A182) [15]. The IMLI blanket is comprised of 10 reflector layers (1/4-mil double-aluminized Mylar) connected together by discrete plastic spacers as previously reported. This test specimen was custom fabricated for precise installation onto the 1-m tall by 167-mm diameter cold mass assembly of the Cryostat-100 test apparatus.

The blanket was initially re-tested for a baseline thermal performance result. Then, 84 nylon pins were inserted all the way through the blanket using a standard garment tagging tool, of which 56 are in the test section of the blanket. The spacing was 76 mm or greater in between pins in both directions. Images of a single pin and the final installation of pins are shown in Figure 1. An image of the coupon after installation is shown in Figure 2.

All tests were conducted in the cold vacuum pressure (CVP) condition of high vacuum ( $<1 \times 10^{-5}$  torr) after a standard round of vacuum-heating purge cycles with a residual gas of nitrogen. The warm and cold boundary temperatures were 293 K and 78 K, respectively, for all tests. The complete test matrix is shown in Table 1. There was a 9% increase in layer density between the initial installation for A164 and the installations for A191 and A192, however, the latter two tests were nearly identical in installation measurements. Further details on the preparation steps and nomenclature are found in ASTM C740. [16]

**Table 1.** Cryostat-100 test matrix and coupon geometries.

Test Series	# layers [n]	Thickness [x] (mm)	Layer Density [z] (layers/mm)*	Effective Area [ $A_e$ ] ( $m^2$ )	CVP Tested (torr)	Warm Boundary Temperature (K)	# pins
A164	10	16.5	0.54	0.334	$\sim 10^{-6}$	$\sim 293$	0
A191	10	15.2	0.59	0.331	$\sim 10^{-6}$	$\sim 293$	0
A192	10	15.1	0.60	0.331	$\sim 10^{-6}$	$\sim 293$	56

\* The layer density is based on nine layers rather than ten layers because the first layer is placed directly onto the cold mass surface without any spacer layer.

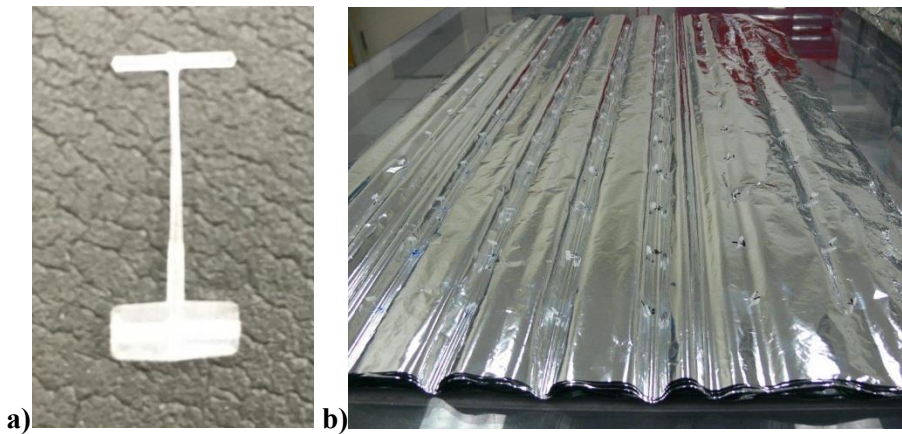


**Figure 1.** Images of a single pin (a) and pins after being installed in the IMLI blanket (b). The test specimen is shown laid flat on the preparation table before installation on the cylindrical cold mass.



**Figure 2.** Image of the coupon with pins after installation onto Cryostat-100.

### 3. Results and Discussion

The cryogenic thermal performance testing results are summarized in Table 2 and Figure 3. Between A164 testing in 2012 and A191 testing in 2015 there was an increase in heat flux of approximately 15 - 20%. This change in the baseline thermal performance may be attributed to the 10% increase in layer density or the slightly higher CVP (lower density MLI blankets are much more susceptible to vacuum pressure changes than higher density blankets). However, there also may have been some minor damage to the blanket by multiple installations and removals. With the pins installed in test specimen A192, the total heat load measured was 0.47 W representing a heat load increase of 0.10 W compared to A191 without the pins after 20 hours, however, after 50 hours of testing, this changed to 0.51 W for A192 compared to 0.35 W for A191 for a heat load increase of 0.16 W. The test and guard boil-off flow rates versus time for A191 and A192 are shown in Figure 4 and Figure 5.

**Table 2.** Cryostat-100 test data for MLI systems with and without pins.

Test Series (Data Time)	CVP (Torr)	WBT (K)	Q (W)	$k_e$ (mW/m/K)	q (W/m <sup>2</sup> )
A164	$5 \times 10^{-6}$	291.7	0.31	0.072	0.92 +/- 0.029
A191 (20 hrs)	$2 \times 10^{-5}$	292.4	0.37	0.078	1.11 +/- 0.036
A191 (50 hrs)	$2 \times 10^{-5}$	293.0	0.35	0.074	1.04 +/- 0.033
A192 (20 hrs)	$7 \times 10^{-6}$	293.3	0.47	0.099	1.41 +/- 0.048
A192 (50 hrs)	$7 \times 10^{-6}$	292.4	0.51	0.106	1.51 +/- 0.048

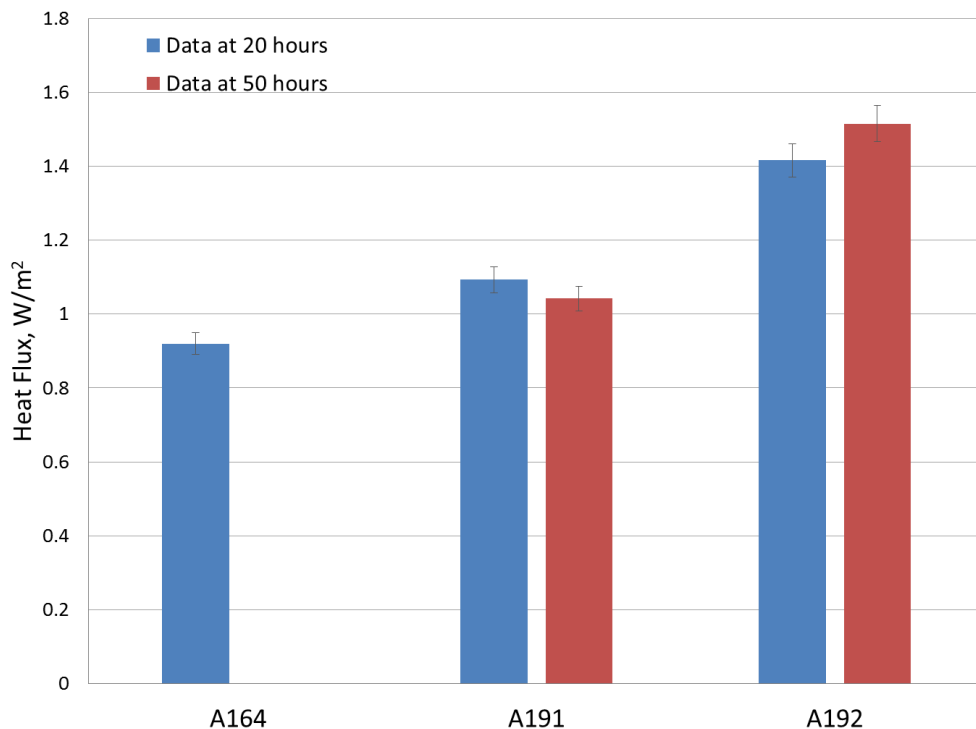


**Figure 3.** Heat flux ( $q$ ) high vacuum for MLI systems with and without pins.

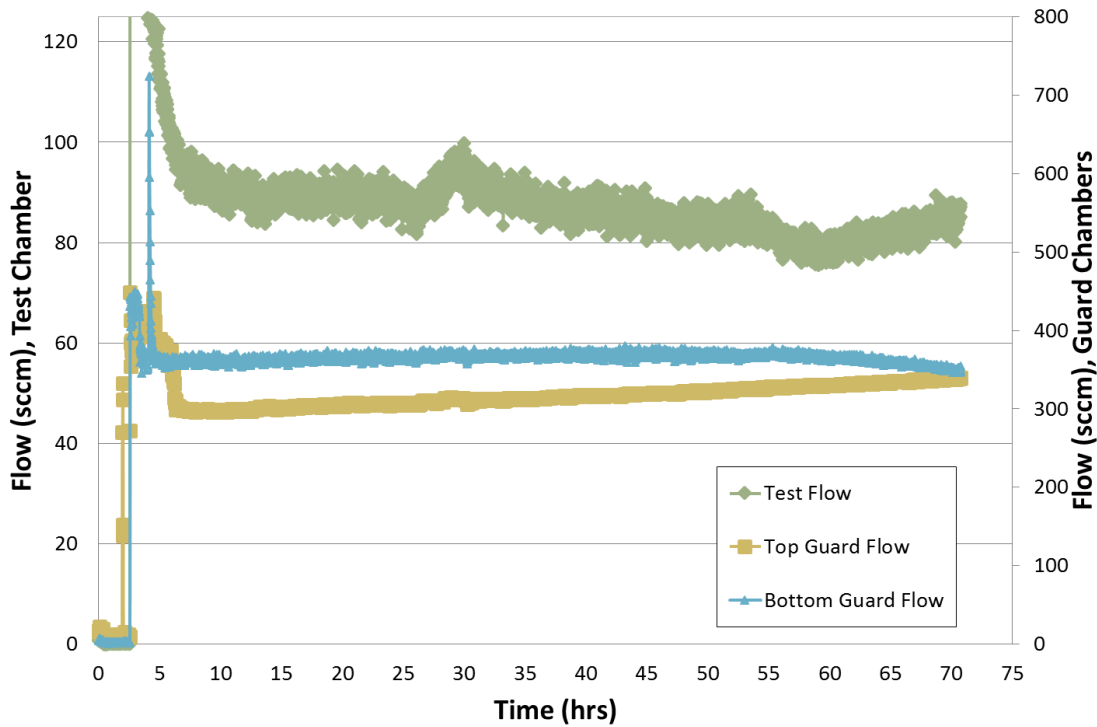


**Figure 4.** Flow rates as a function of time for A191.

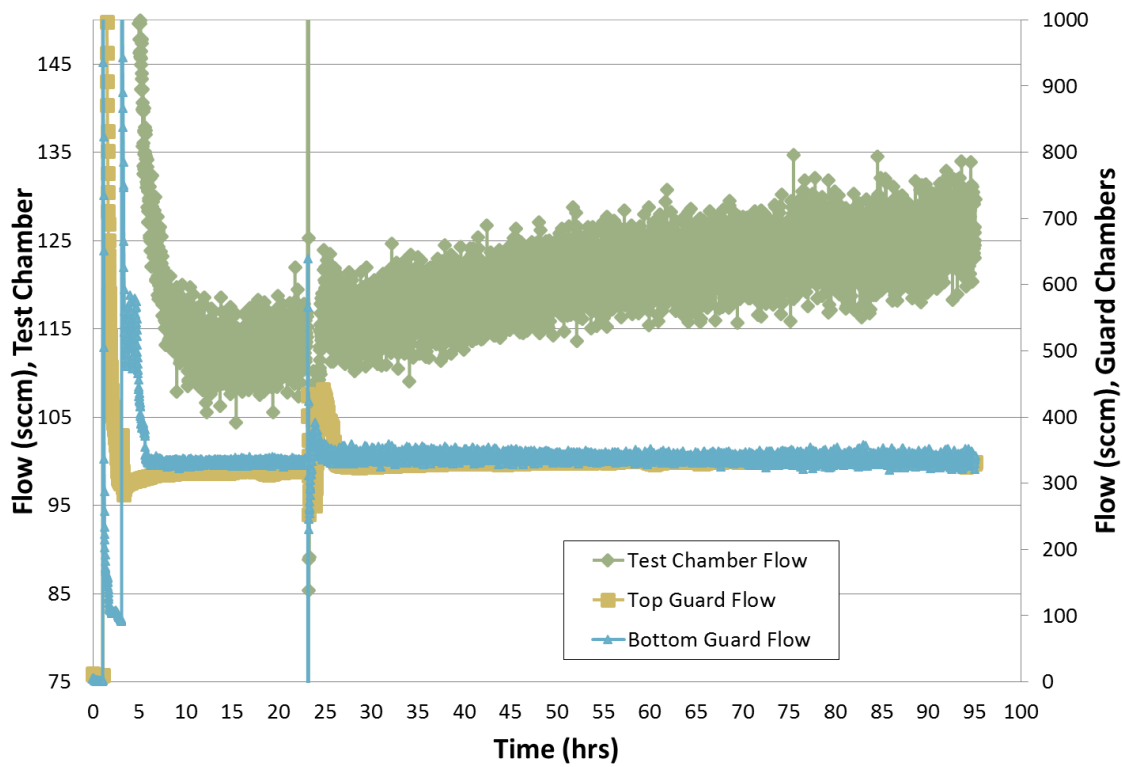


**Figure 5.** Flow rates as a function of time for A192.

Based on the actual size of the pin (as shown in Figure 1), a new expected conduction heat load was calculated. The cross sectional area varied with linear diameter from 0.27 mm on the cold side to 0.85 mm on the warm side, the length of the pin was the thickness of the blanket or 15.1 mm, and the thermal conductivity for Nylon was used from NIST. [17] For 56 pins, the expected heat load was 46 mW, or 0.83 mW per pin. However, this solid conduction heat load would be for perfect thermal contact between a given pin and the cold mass surface. If the inner surface of the MLI is at 160 K (the temperature needed to have a radiative heat flux of 1.1 W/m<sup>2</sup> to the cold mass), this drops to 0.52 mW per pin or 29 mW total.

#### 4. Performance Modelling

Initially, it was assumed that the conduction through the pins would dominate the heat transfer associated with the penetration. However, based on the calculations and results from both this effort and Black, that assumption was revisited. Direct radiation through the hole created can be easily estimated using an emissivity of 1 (both warm and cold surfaces were painted black with emissivity of 0.95) as being on the order of 0.3 mW per hole (assuming just larger than the 0.8 mm diameter hole). However, for perforated MLI, Fox, Keifel, and McIntosh developed a different theory based on the view factors of each perforation or hole referencing data from Eckert. [18, 19] They showed that by taking a 10 degree angle from the point source, the effective radiation area was much larger than just the hole size (see Figure 6). This allows the effect of perforation size and spacing to be accounted for as shown in Tien. [20]. For example, the same analysis shows that for similar MLI blankets with 2% total open area, the heat flux increase due to smaller size holes (~1 mm) is twice that due to larger size holes (~10 mm).

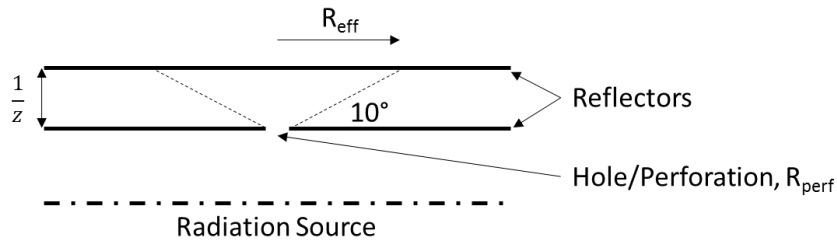


**Figure 6.** Diagram of effective radiation area.

The effective radius ( $r_{eff}$ ) can be shown mathematically as:

$$r_{eff} = \frac{1}{z \tan \theta} + r_{perf} \quad (1)$$

Where  $z$  is the layer density,  $r_{perf}$  is the radius of the hole, and  $\theta$  is assumed to be 10 deg (0.175 rad). The total heat load due to the penetration can then be modeled as:

$$\dot{Q} = A_{eff} \epsilon_{layer} \sigma (T_h^4 - T_c^4) + \int \frac{A}{dx} \int k dT \quad (2)$$

Where  $A_{eff}$  is the effective area,  $\epsilon_{layer}$  is the emissivity of an individual layer,  $\sigma$  is the Stefan-Boltzman constant ( $5.67 \times 10^{-8} \text{ W/m}^2/\text{K}^4$ ),  $T_h$  is the warm environmental temperature (not the temperature of the outer layer), and  $T_c$  is the cold environmental temperature. The two integrals account for the conduction down the pin (the first accounts for the variable geometry, the second for the variable thermal conductivity). Results for multiple test results from this approximation are shown in Table 3.

**Table 3:** Comparison of predicted and measured heat load for pin tests.

Test Series	Hole Radius (mm)	# layers	Layer Density (lay/mm)	$Q_{\text{hole}}$ (mW)	$Q_{\text{pin}}$ (mW)	$Q_{\text{total}}$ (mW)	$Q_{\text{meas}}$ (mW)
A192	0.5	10	0.6	3.1	0.52	3.6	2.0-2.8
Black [9]	0.5	10	1.3	3.3	0.3	3.6	~3

The comparison between the predicted and measured values is within 50%. It should also be noted that the  $r_{\text{eff}}$  for A192 is approximately 9 mm, which is much less than the 75 mm spacing of the penetrations.

## 5. Conclusions

Testing was performed on a sample with multiple small penetrations such as pins, tags, or stitches that may go through an MLI blanket for installation. This approach allowed the heat gain through the blanket to be measurable while the small penetration (pins) were far enough apart to not have overlapping effects. A method of analysis was shown to match the results within 50%. The test methodology and direct heat flow rate measurements allow engineers to estimate heat loads through a blanket due to small penetrations that are often needed to hold an MLI blanket onto a tank. While this blanket is not traditional in nature, since the main effects are radiation through the hole and conduction down the pin, for fine netting or fiberglass that is mostly transparent to radiation, the effects should hold. The intended use of this is to give engineers a method by which to directly predict the heat load and weigh the structural benefits vs thermal penalties of adding multiple small penetrations for specific designs.

## References

- [1] L.D. Stimpson and W. Jaworski, "Effects of Overlaps, Stitches, and Patches on Multilayer Insulation", AIAA 72-285.
- [2] K. E. Leonard, Cryogenic Insulation Development, Final Report, NASA CR-123938, 1972.
- [3] E. H. Hyde, Multilayer Insulation Thermal Protection Systems Technology, Research Achievements IV NASA TM X-64561, 1971, pp. 5-52.
- [4] C.W. Keller, G.R. Cunningham, et al., Thermal Performance of Multi-layer Insulations, Final Report, NASA CR-134477, 1974.
- [5] R. A. Mohling, H. L. Geir, et al., Multilayer Insulation Thich Blanket Performance Demonstration, AFAL TR-87-037, Ball Aerospace Systems Group, Boulder, CO, July 1987.
- [6] W.L. Johnson, A.O. Kelly, et. al. Two Dimensional Heat Transfer around Penetrations in Multilayer Insulation, NASA-TP-2012-216315, 2012.
- [7] Q.S. Shu, R.W. Fast, and H.L. Hart, "Systematic Study to Reduce the Effects of Cracks in Multilayer Insulation Part 2: Experimental Results". Cryogenics, Vol 27, pp. 298-311. 1987.
- [8] R.B. Hinckley, *Liquid Propellant Losses During Space Flight, Final Report*. NASA-CR-53336, Arthur D. Little, Inc, Cambridge, MA. 1964
- [9] I.A. Black, P.E. Glaser, and R.C. Reid, "Heat Loss Through Evacuated Multilayer Insulation Penetrated By a Low-Conductivity Pin", Bull. IIR, Annex 1966-2, 233-243 (Meeting Of Commission 2, Trondheim, Norway, Jun 22-24, 1966).
- [10] J.E. Fesmire, W.L. Johnson, B. Meneghelli, and B.E. Coffman, "Cylindrical boiloff calorimeters for testing of thermal insulations," IOP Conf. Series: Materials Science and Engineering 101 (2015).
- [11] W.L. Johnson, Thermal Performance of Cryogenic Multilayer Insulation at Various Layer Spacings, Master's Thesis, University of Central Florida, Dec. 2010.
- [12] J.E. Fesmire, "Standardization in cryogenic insulation systems testing and performance data," International Cryogenic Engineering Conference - 25, Enschede Netherlands, July 2014.
- [13] ASTM C1774 - *Standard Guide for Thermal Performance Testing of Cryogenic Insulation Systems*. ASTM International, West Conshohocken, PA, USA (2013).
- [14] W.L. Johnson, K.W. Heckle, and J. Hurd, "Thermal coupon testing of Load-Bearing Multilayer Insulation", *AIP Conference Proceedings 1573*, pg. 725, 2014.
- [15] W.L. Johnson, J.E. Fesmire, and K.W. Heckle, "Demonstration of Hybrid Multilayer Insulation of Fixed Thickness Applications", *IOP Conf. Ser.: Mater. Sci. Eng.* **101** 012015, 2015.
- [16] ASTM C740 - *Standard Guide for Evacuated Reflective Cryogenic Insulation*. ASTM International, West Conshohocken, PA, USA (2013).

- [17] NIST Thermal Physical Properties, <https://www.nist.gov/mml/acmd/structural-materials-group/cryogenic-material-properties-index>.
- [18] E.C. Fox, E.R. Keifel, and G.L. McIntosh, et.al. "Multipurpose Hydrogen Test Bed System Definition and Insulated Tank Development", Martin Marietta Astronautics, NASA CR-194355, July 1993.
- [19] E.R.G. Eckert, *Introduction to the Transfer of Heat and Mass*, McGraw-Hill, NY, 1950, pg 203.
- [20] C.L. Tien and G.R. Cunnington, "Radiation Heat Transfer in Multilayer Insulation Having Perforated Shields", Presented at the AIAA 8<sup>th</sup> Thermophysics Conference, AIAA 73-718, 1973

### **Acknowledgements**

This work was supported by the National Aeronautics and Space Administration's Evolvable Cryogenics Technology Demonstration Mission.